

## Research Article

# Sparsity-Preserving Two-Sided Iterative Algorithm for Riccati-Based Boundary Feedback Stabilization of the Incompressible Navier–Stokes Flow

Md. Toriql Islam <sup>1</sup>, Mahtab Uddin <sup>1,2</sup>, M. Monir Uddin <sup>3</sup>, Md. Abdul Hakim Khan <sup>1</sup>  
and Md. Tanzim Hossain <sup>4</sup>

<sup>1</sup>Department of Mathematics, Bangladesh University of Engineering Technology, Dhaka 1000, Bangladesh

<sup>2</sup>Institute of Natural Sciences, United International University, Dhaka 1212, Bangladesh

<sup>3</sup>Department of Mathematics and Physics, North South University, Dhaka 1229, Bangladesh

<sup>4</sup>Department of Electrical and Computer Engineering, North South University, Dhaka 1229, Bangladesh

Correspondence should be addressed to Mahtab Uddin; mahtab@ins.uui.ac.bd

Received 14 April 2022; Accepted 14 October 2022; Published 22 November 2022

Academic Editor: Eric Campos

Copyright © 2022 Md. Toriql Islam et al. This is an open access article distributed under the Creative Commons Attribution License, which permits unrestricted use, distribution, and reproduction in any medium, provided the original work is properly cited.

In this paper, we explore the Riccati-based boundary feedback stabilization of the incompressible Navier–Stokes flow via the Krylov subspace techniques. Since the volume of data derived from the original models is gigantic, the feedback stabilization process through the Riccati equation is always infeasible. We apply a  $\mathcal{H}_2$  optimal model-order reduction scheme for reduced-order modeling, preserving the sparsity of the system. An extended form of the Krylov subspace-based two-sided iterative algorithm (TSIA) is implemented, where the computation of an equivalent Sylvester equation is included for minimizing the computation time and enhancing the stability of the reduced-order models with satisfying the Wilson conditions. Inverse projection approaches are applied to get the optimal feedback matrix from the reduced-order models. To validate the efficiency of the proposed techniques, transient behaviors of the target systems are observed incorporating the tabular and figurative comparisons with MATLAB simulations. Finally, to reveal the advancement of the proposed techniques, we compare our work with some existing works.

## 1. Introduction

In the present day, the incompressible Navier–Stokes flow is one of the most impressive contents of interest of the researchers. It has a prominent impact on fluid mechanics, naval engineering, oceanography, and water resource scientists. In the analysis of fluid properties and attributes of undersea atmospheres, the incompressible Navier–Stokes flow is one of the prominent issues for naval architects. It is an essential part of the investigation of sea-route analysts.

Details of the Navier–Stokes equations with the discretization can be found in references [1, 2]. Linearizing the Navier–Stokes equations in space and time variables by a mixed finite element method without altering the time

variable converts them into linear time-invariant systems [3]. The incompressible Navier–Stokes flow can be written as the following differential-algebraic equations:

$$\begin{aligned} M\dot{v}(t) &= A_1v(t) + A_2p(t) + B_1u(t), \\ 0 &= A_3v(t) + B_2u(t), \\ y(t) &= C_1v(t) + C_2p(t) + Du(t), \end{aligned} \quad (1)$$

where  $v(t) \in \mathbb{R}^{n_v}$  is the nodal vector of the discretized velocity with  $v(0) = v_0$ ,  $p(t) \in \mathbb{R}^{n_p}$  is the discretized pressure, and  $u(t) \in \mathbb{R}^{n_u}$  is the input with the output  $y(t) \in \mathbb{R}^{n_y}$ . The symmetric positive definite matrix  $M \in \mathbb{R}^{n_v \times n_v}$  represents the mass, whereas the matrices  $A_1 \in \mathbb{R}^{n_v \times n_v}$ ,  $A_2 \in \mathbb{R}^{n_v \times n_p}$ , and  $A_3 \in \mathbb{R}^{n_p \times n_v}$  are for system components including discretized

gradient.  $B_1 \in \mathbb{R}^{n_v \times n_u}$  and  $B_2 \in \mathbb{R}^{n_p \times n_u}$  are the input matrices, whereas  $C_1 \in \mathbb{R}^{n_v \times n_v}$  and  $C_2 \in \mathbb{R}^{n_p \times n_p}$  are the output matrices. The input-output matrices quantify the velocity pattern at the corresponding nodes.  $D \in \mathbb{R}^{n_v \times n_u}$  is the direct transform matrix [4]. Considering  $M$  is invertible,  $A_2$  and  $A_3$  have both full column ranks and  $A_3 M^{-1} A_2$  is nonsingular. Hence, system (1) is of the index-2 differential-algebraic system having the dimension  $n_v + n_p$  [5]. A system equivalent to system (1) can be written in the following form:

$$\begin{aligned} \bar{E}\dot{x}(t) &= \bar{A}x(t) + \bar{B}u(t), \\ y(t) &= \bar{C}x(t) + \bar{D}u(t), \end{aligned} \quad (2)$$

where  $x(t) = \begin{bmatrix} v(t) \\ p(t) \end{bmatrix}$ ,  $\bar{E} = \begin{bmatrix} M & 0 \\ 0 & 0 \end{bmatrix}$ ,  $\bar{A} = \begin{bmatrix} A_1 & A_2 \\ A_3 & 0 \end{bmatrix}$ ,  $\bar{B} = [B_1 \ B_2]$ ,  $\bar{C} = \begin{bmatrix} C_1 \\ C_2 \end{bmatrix}$ , and  $\bar{D} = D$  with appropriate dimensions. The matrix pencil corresponding to the system is defined as  $(\bar{A}, \bar{E})$ , where the matrix  $\bar{E}$  is singular and the matrix pencil  $(\bar{A}, \bar{E})$  has  $n_v - n_p$  number of nonzero finite complex eigenvalues and  $2n_p$  infinite eigenvalues [6].

Reynolds number (Re) is one of the key features that instigate the system characteristics. For  $\text{Re} \geq 300$ , the Navier–Stokes flow turns unstable and analysis of the flow attributes becomes troublesome [7]. Optimal feedback stabilization of the Navier–Stokes flow is indispensable and Riccati-based boundary feedback stabilization is the best apparatus in this situation [8]. The Riccati equation corresponding to the system (2) is of the form:

$$\bar{A}^T X \bar{E} + \bar{E}^T X \bar{A} - \bar{E}^T X \bar{B} \bar{B}^T X \bar{E} + \bar{C}^T \bar{C} = 0. \quad (3)$$

The solution  $X$  of the Riccati equation (3) is symmetric positive definite and called stabilizing for a stable closed-loop matrix  $\bar{A} - (\bar{B} \bar{B}^T)^T X \bar{E}$ . The optimal feedback matrix  $K^o$  can be computed as  $K^o = \bar{B}^T X \bar{E}$  and can be implemented for optimally stabilizing the target system by replacing  $\bar{A}$  by  $\bar{A}_s = \bar{A} - \bar{B} K^o$  [9]. The stabilized system can be written as follows:

$$\begin{aligned} \bar{E}_s \dot{x}(t) &= \bar{A}_s x(t) + \bar{B} u(t), \\ y(t) &= \bar{C} x(t) + \bar{D} u(t). \end{aligned} \quad (4)$$

With the increasing number of flow components and finer meshes in the discretization process, the dimensions of the matrices in system (1) become very large. Due to the size of the system matrices, Riccati-based boundary feedback stabilization of system (1) is infeasible as the associated Riccati equation cannot be solved by the usual matrix equation solvers [10]. To overcome this adversity, a suitable model-order reduction (MOR) technique needs to be applied [11]. A computationally convenient reduced-order model (ROM) of system (2) can be written as follows:

$$\begin{aligned} \hat{\bar{E}} \hat{x}(t) &= \hat{\bar{A}} \hat{x}(t) + \hat{\bar{B}} \hat{u}(t), \\ \hat{y}(t) &= \hat{\bar{C}} \hat{x}(t) + \hat{\bar{D}} \hat{u}(t). \end{aligned} \quad (5)$$

where  $\hat{\bar{E}} = W^T \bar{E} V$ ,  $\hat{\bar{A}} = W^T \bar{A} V$ ,  $\hat{\bar{B}} = W^T \bar{B}$ ,  $\hat{\bar{C}} = \bar{C} V$ , and  $\hat{\bar{D}} = \bar{D}$ . The projector  $V$  and  $W$  can be found in any compatible MOR technique [12]. Using the reduced-order matrices given in formula (5), the reduced-order form of Riccati equation (3) can be obtained as follows:

$$\hat{\bar{A}}^T \hat{X} \hat{\bar{E}} + \hat{\bar{E}}^T \hat{X} \hat{\bar{A}} - \hat{\bar{E}}^T \hat{X} \hat{\bar{B}} \hat{\bar{B}}^T \hat{X} \hat{\bar{E}} + \hat{\bar{C}}^T \hat{\bar{C}} = 0. \quad (6)$$

Now, the optimal feedback matrix for system (2) can be approximated by applying the ROM (5). The reduced-order Riccati equation (6) is to be solved for a symmetric positive-definite matrix  $\hat{X}$  by the MATLAB library command *care*. Then, the stabilizing feedback matrix  $\hat{K} = \hat{\bar{B}}^T \hat{X} \hat{\bar{E}}$  corresponding to the ROM (5) can be estimated, and hence, the approximated optimal feedback matrix  $K^o = \hat{K} V^T \bar{E}$  [13]. Finally, utilizing  $K^o$  stabilization of system (2) can be carried out as system (4).

There are a number of MOR techniques that currently exist and are in use, namely, singular value decomposition (SVD)-based balanced truncation (BT) and Krylov subspace-based iterative rational Krylov algorithm (IRKA). Those techniques are elaborately discussed in references [8, 14–21] and references therein. From the discussion of the BT method, some obstacles are identified, such as its demands to solve two large-dimensional Lyapunov equations for controllability and observability Gramian, which is very costly for computational time and memory requirements. On the other hand, IRKA is better in the sense of simulation time and needs less memory allocation but the stability of the ROM is not guaranteed. For solving the Riccati equation without explicit estimation of the ROM, some techniques are available in practice, for example, low-rank alternative direction implicit (LR-ADI), integrated Newton–Kleinman (NK) method, and Krylov subspace associated rational Krylov subspace method (RKSM). Those methods are derived and analyzed in detail in references [22–25] and references therein. The Newton–Kleinman method is a very complex approach and at each Newton step, LR-ADI iterations need to be executed once, which is a very time-laborious task [26–29]. Also, the Newton–Kleinman method cannot ensure the definiteness of the solution of the Riccati equation derived from an unstable system. On the contrary, RKSM is straightforward for simulation but lack of proper shift parameter selection sometimes makes this method ineffective and adjustment of the stopping criteria may encounter the convergence of the method. An initial feedback matrix can be a remedy for unstable systems in the RKSM approach but this additional step makes the total process inconvenient in the sense of time management [30].

To overcome abovementioned troubles and complexities, we are proposing an extended form of Krylov subspace-based two sided iterative algorithm (TSIA) as discussed in references [31–33] and references therein. In this strategy, initially, we need to find a ROM of the target model implementing any conventional technique, then two generalized sparse-dense Sylvester equations will be solved to find the system Gramian; hence, the required projection matrices constituted by their orthonormal columns constructed via QZ-decomposition [34]. The ROM attained by

the TSIA approach is stability-preserving and we will derive its sparsity-preserving form of it. Then, rest of the activities will follow the classical inverse projection scheme discussed previously. The validity of the proposed techniques will be investigated numerically through the transient behavior of the target models and accuracy will be justified by the  $\mathcal{H}_2$  norm optimality.

## 2. Background

Here, we discuss the basic approaches for the treatment of a generalized state-space system. Then, we briefly analyze the conversion of index-2 descriptor systems into equivalent generalized systems with several cases. At the end of this section, we investigate sparsity-preserving reduced-order matrices and the corresponding reduced-order model. The generalized state-space system can be written as follows:

$$\begin{aligned} E\dot{x}(t) &= Ax(t) + Bu(t), \\ y(t) &= Cx(t) + Du(t), \end{aligned} \quad (7)$$

where  $E \in \mathbb{R}^{n \times n}$  is nonsingular, and  $A \in \mathbb{R}^{n \times n}$ ,  $B \in \mathbb{R}^{n \times p}$ ,  $C \in \mathbb{R}^{m \times n}$ , and  $D \in \mathbb{R}^{m \times p}$ . The transfer function of system (7) is defined by  $G(s) = C(sE - A)^{-1}B + D$ , where  $s \in \mathbb{C}$ . The CARE defined for system (7) is as follows:

$$A^T X E + E^T X A - E^T X B B^T X E + C^T C = 0. \quad (8)$$

**2.1. Newton–Kleinman Method.** The Newton–Kleinman method is used to convert the Riccati equation to an equivalent Lyapunov equation and to thereby solve this Lyapunov equation by a suitable strategy.

According to the Fre'chet derivative at  $X = X_i$  and applying the Newton iteration with the condition  $\Delta X_i = X_{i+1} - X_i$ , we obtain the following:

$$\begin{aligned} (A - B B^T X_i E)^T X_{i+1} E + E^T X_{i+1} (A - B B^T X_i E) \\ = -C^T C - E^T X_i B B^T X_i E. \end{aligned} \quad (9)$$

Now, we consider  $\tilde{A}_i = A - B B^T X_i E$  and  $\mathcal{W}_i = \begin{bmatrix} C^T & E^T X_i B \end{bmatrix}$ , then formula (9) reduces to a generalized Lyapunov equation such as follows:

$$\tilde{A}_i^T X_{i+1} E + E^T X_{i+1} \tilde{A}_i = -\mathcal{W}_i \mathcal{W}_i^T. \quad (10)$$

The generalized CALE (10) can be solved for  $X_{i+1}$  by any conventional method, and the corresponding feedback matrix  $K_{i+1} = B^T X_{i+1} E$  can be estimated [35]. The summary of the method is given in Algorithm 1.

The solution of the generalized CALE (10) can be found through the Cholesky factorization utilizing the low-rank Cholesky-factor alternative direction implicit (LRCF-ADI) techniques. Details of the LRCF-ADI techniques are provided in references [36–38] and references therein. In this approach, only the Cholesky factor  $Z$  of the solution  $X$  in needs to store. The summary of LRCF-ADI techniques is given in Algorithm 2.

**2.2. Rational Krylov Subspace Algorithm.** The rational Krylov subspace algorithm is applicable to find the factored solution of CARE (8) without any conversion. This algorithm is defined for the LTI systems of symmetric cases. An orthogonal projector  $V \in \mathbb{R}^{n \times m}$  spanned by the  $m$ -dimensional rational Krylov subspace needs to construct for finding the an approximated low-rank CARE defined as follows:

$$\hat{A}^T \hat{X} \hat{E} + \hat{E}^T \hat{X} \hat{A} - \hat{E}^T \hat{X} \hat{B} \hat{B}^T \hat{X} \hat{E} + \hat{C}^T \hat{C} = 0, \quad (11)$$

where  $\hat{X} = V^T X V$ ,  $\hat{E} = V^T E V$ ,  $\hat{A} = V^T A V$ ,  $\hat{B} = V^T B$  and  $\hat{C} = C V$ . The low-rank CARE (11) can be solved for  $\hat{X} \in \mathbb{R}^{m \times m}$  by any conventional method or MATLAB *care* command, where  $\hat{X}$  is taken as a low-rank approximation of  $X$ . Then, the factored solution  $Z$  of the solution  $X$  is estimated to find the optimal feedback matrix  $K^o$ .

The derivation and update of the RKSM techniques are given in references [39, 40] and references therein. The step-by-step RKSM approach is given in [41] and summarized in Algorithm 3.

**2.3. Iterative Rational Krylov Algorithm.** Iterative rational Krylov algorithm (IRKA) can be applied to construct an  $r$ -dimensional ( $r \ll n$ ) reduced-order model

$$\begin{aligned} \hat{E} \hat{x}(t) &= \hat{A} \hat{x}(t) + \hat{B} \hat{u}(t), \\ \hat{y}(t) &= \hat{C} \hat{x}(t) + \hat{D} \hat{u}(t), \end{aligned} \quad (12)$$

such that its transfer function  $\hat{G}(s) = \hat{C}(s\hat{E} - \hat{A})^{-1}\hat{B} + \hat{D}$  interpolates the original one,  $G(s)$ , at selected points in the complex plane along with selected directions. The detailed procedure of IRKA is illustrated in reference [42].

Via the IRKA approach, two projection matrices  $V$  and  $W$  are to be constructed; hence, by the Petrov–Galerkin condition, we can construct the reduced-order matrices in formula (12) as follows:

$$\hat{E} = W^T E V, \hat{A} = W^T A V, \hat{B} = W^T B, \hat{C} = C V, \hat{D} = D. \quad (13)$$

Using the reduced-order matrices defined in formula (13), the reduced-order CARE can be attained as formula (11) and can be solved for  $\hat{X}$  as previously. Then, the stabilizing feedback matrix  $\hat{K} = \hat{B}^T \hat{X} \hat{E}$  corresponding to the ROM (12) can be estimated; hence, for stabilizing the full model (7), the approximated optimal feedback matrix  $K^o$  can be retrieved by the scheme of reverse projection as follows:

$$K^o = \left( \hat{B}^T \hat{X} \hat{E} \right) V^T E = \hat{K} V^T E. \quad (14)$$

The iterative rational Krylov algorithm (IRKA) introduced in reference [43] resolves the problem by iteratively correcting the interpolation points and the directions as summarized in Algorithm 4.

**2.4. Conversion of the Index-2 Descriptor System to Generalized System.** Let us Assume  $M$  is a nonsymmetric positive definite and  $A_2^T \neq A_3$ . Initially, we consider  $B_2 = 0$ . According to Section 3 of reference [44], the algebraic part of

Input:  $E, A, B, C$  and  $X_0$  (initial assumption).  
 Output: approximate feedback matrix  $K$

- (1) While  $i \leq i_{\max}$  do
- (2) Compute  $A_i = A - BB^T X_i E$  and  $\mathcal{W}_i = [C^T E^T X_i B]$ .
- (3) Solve the Lyapunov (10) for  $X_{i+1}$ .
- (4) Compute  $K_{i+1} = B^T X_{i+1} E$ .
- (5) end while.

ALGORITHM 1: Basic Kleinman–Newton method

Input:  $E, A, C, \tau$  (tolerance),  $i_{\max}$  (number of iterations) and shift parameters  $\{\mu_j\}_{j=1}^{i_{\max}}$ .  
 Output: low-rank Cholesky-factor  $Z$  such that  $X \approx ZZ^T$ .

- (1) Consider  $\mathcal{W}_0 = C^T, Z_0 = \emptyset$ , and  $i = 1$ .
- (2) while  $\|\mathcal{W}_{i-1} \mathcal{W}_{i-1}^T\| \geq \tau$  or  $i \leq i_{\max}$  do
- (3) Solve  $\mathcal{V}_i = (\tilde{A}^T + \mu_i E^T)^{-1} \mathcal{W}_{i-1}$ .
- (4) if  $\text{Im}(\mu_i) = 0$  then
- (5) Update  $Z_i = [Z_{i-1} \sqrt{-2\mu_i} \mathcal{V}_i]$ ,
- (6) Compute  $\mathcal{W}_i = \mathcal{W}_{i-1} - 2\mu_i E^T \mathcal{V}_i$ .
- (7) else
- (8) Assume  $\gamma_i = \sqrt{-2\text{Re}(\mu_i)}$ ,  $\delta_i = \text{Re}(\mu_i)/\text{Im}(\mu_i)$ ,
- (9) Update  $Z_{i+1} = [Z_{i-1} \gamma_i (\text{Re}(\mathcal{V}_i) + \delta_i \text{Im}(\mathcal{V}_i)) \gamma_i \sqrt{\delta_i^2 + 1} \text{Im}(\mathcal{V}_i)]$ ,
- (10) Compute  $\mathcal{W}_{i+1} = \mathcal{W}_{i-1} + 2\gamma_i^2 E^T [\text{Re}(\mathcal{V}_i) + \delta_i \text{Im}(\mathcal{V}_i)]$ .
- (11)  $i = i + 1$
- (12) end if
- (13)  $i = i + 1$
- (14) end while.

ALGORITHM 2: LRCF-ADI for generalized systems

Input:  $E, A, B, C, i_{\max}$  (number of iterations) and  $\mu_i$  (initial shifts).  
 Output: optimal feedback matrix  $K^o$

- (1) Compute  $Q_0 R_0 = C^T$  (QR factorization).
- (2) Choose  $V_0 = Q_0$ .
- (3) while not converged or  $m \leq i_{\max}$  do
- (4) Solve  $v_{m+1} = (A^T - \mu_{m+1} E^T)^{-1} V_m$ .
- (5) Compute shift for the next iteration.
- (6) Using the Arnoldi algorithm orthogonalize  $v_{m+1}$  against  $V_m$  to obtain  $\hat{v}_{m+1}$ , such that  $V_{m+1} = [V_m, \hat{v}_{m+1}]$ .
- (7) Assuming  $\hat{E} = V_{m+1}^T E V_{m+1}$ ,  $\hat{A} = V_{m+1}^T A V_{m+1}$ ,  $\hat{B} = V_{m+1}^T B$  and  $\hat{C} = C V_{m+1}$ , for  $\hat{X}$  solve the Riccati (11).
- (8) Compute  $\|\mathcal{R}_m\|_{(\text{relative})}$  for convergence.
- (9) end while
- (10) Compute eigenvalue decomposition  $\hat{X} = T \Lambda T^T = [T_1 \ T_2] \begin{bmatrix} \Lambda_1 & 0 \\ 0 & \Lambda_2 \end{bmatrix} \begin{bmatrix} T_1^T \\ T_2^T \end{bmatrix}$ .
- (11) For negligible eigenvalues truncate  $\Lambda_2$  and compute  $Z = V_{m+1} T_1 \Lambda_1^{1/2}$ .
- (12) Compute  $K^o = B^T (ZZ^T) E$ .

ALGORITHM 3: RKSM for generalized systems.

the system (1),  $p(t)$  can be expressed as  $v(t)$ . Then, by proper elimination and substitution, system (1) can be converted to an equivalent form:

$$\begin{aligned} \mathcal{E} \dot{x}(t) &= \mathcal{A} x(t) + \mathcal{B} u(t), \\ y(t) &= \mathcal{C} x(t) + \mathcal{D} u(t), \end{aligned} \quad (15)$$

where the converted matrices are structured as follows:

$$\begin{aligned} x &= x_1, \quad \mathcal{E} = \Pi_l M \Pi_r, \quad \mathcal{A} = \Pi_l A_1 \Pi_r, \quad \mathcal{B} = \Pi_l B_1, \\ \mathcal{C} &= \left( C_1 - C_2 (A_3 M^{-1} A_2)^{-1} A_3 M^{-1} A_1 \right) \Pi_r, \end{aligned} \quad (16)$$

$$\mathcal{D} = D - C_2 (A_3 M^{-1} A_2)^{-1} A_3 M^{-1} B_1,$$

with  $\Pi_l^T v(0) = \Pi_l^T v_0$ . The projectors  $\Pi_l$  and  $\Pi_r$  are composed as follows:

Input:  $E, A, B, C, D$

Output: optimal feedback matrix  $K^o$ .

- (1) Make the initial selection of the interpolation points  $\{\alpha_i\}_{i=1}^r$  and the tangential directions  $\{b_i\}_{i=1}^r$  and  $\{c_i\}_{i=1}^r$ .
- (2) Construct the projection matrices  $V = [(\alpha_1 E - A)^{-1} B b_1, \dots, (\alpha_r E - A)^{-1} B b_r]$ ,  $W = [(\alpha_1 E - A)^{-T} C^T c_1, \dots, (\alpha_r E - A)^{-T} C^T c_r]$ .
- (3) while (not converged) do
- (4) Compute the reduced-order matrices as (13).
- (5) Compute  $\tilde{A} z_i = \lambda_i \tilde{E} z_i$  and  $y_i^* \tilde{A} = \lambda_i y_i^* \tilde{E}$  for  $\alpha_i \leftarrow -\lambda_i$ ,  $b_i^* \leftarrow -y_i^* \tilde{B}$  and  $c_i^* \leftarrow \tilde{C} z_i^*$ , for  $i = 1, \dots, r$ .
- (6) Repeat step 2.
- (7) Repeat step 4.
- (8) Solve the Riccati (11) for  $\tilde{X}$ .
- (9) Compute  $\tilde{K} = \tilde{B}^T \tilde{X} \tilde{E}$  and hence  $K^o = \tilde{K} V^T E$ .
- (10) end while.

ALGORITHM 4: IRKA for generalized systems.

$$\begin{aligned} \Pi_l &= I - M^{-1} A_2 (A_3 M^{-1} A_2)^{-1} A_3, \\ \Pi_r &= I - A_2 (A_3 M^{-1} A_2)^{-1} A_3 M^{-1}. \end{aligned} \quad (17)$$

For the general case, we assume  $B_2 \neq 0$ . According to Section of reference [45], we consider the velocity  $v(t)$  can be decomposed as follows:

$$v(t) = v_0(t) + v_g(t), \quad (18)$$

where  $v_0(t)$  satisfies  $A_3 v_0(t) = 0$  and  $v_g(t) = M^{-1} A_2 (A_3 M^{-1} A_2)^{-1} B_2 u(t)$ . Thus, the required converted system can be formed as follows:

$$\begin{aligned} \mathcal{E} \dot{x}(t) &= \mathcal{A} x(t) + \mathcal{B} u(t), \\ y(t) &= \mathcal{C} x(t) + \mathcal{D} u(t) - C_2 (A_3 M^{-1} A_2)^{-1} B_2 u(t), \end{aligned} \quad (19)$$

with  $\Pi_l^T v(0) = \Pi_l^T (v_0 + v_g(0))$  and the converted matrices are as follows:

$$\begin{aligned} x &= x_1, \quad \mathcal{E} = \Pi_l M \Pi_r, \quad \mathcal{A} = \Pi_l A_1 \Pi_r, \\ \mathcal{B} &= \Pi_l (B_1 - A_1 M^{-1} A_2 (A_3 M^{-1} A_2)^{-1} B_2), \\ \mathcal{C} &= (C_1 - C_2 (A_3 M^{-1} A_2)^{-1} A_3 M^{-1} A_1) \Pi_r, \\ \mathcal{D} &= D - C_2 (A_3 M^{-1} A_2)^{-1} A_3 M^{-1} B_1. \end{aligned} \quad (20)$$

In addition, if both  $B_2 = 0$  and  $C_2 = 0$ , the converted system will be the same as a system (15) but converted matrices will have the following form:

$$\begin{aligned} x &= x_1, \quad \mathcal{E} = \Pi_l M \Pi_r, \quad \mathcal{A} = \Pi_l A_1 \Pi_r, \\ \mathcal{B} &= \Pi_l B_1, \quad \mathcal{C} = C_1 \Pi_r, \quad \mathcal{D} = D. \end{aligned} \quad (21)$$

According to the formulation derived in Section 4.1 of reference [46], sparsity-preserving reduced-order matrices for the index-2 descriptor systems can be written as follows:

$$\begin{aligned} \tilde{\mathcal{E}} &= W^T M V, \quad \tilde{\mathcal{A}} = W^T A_1 V, \\ \tilde{\mathcal{B}} &= W^T B_1 - (W^T A_1) M^{-1} A_2 (A_3 M^{-1} A_2)^{-1} B_2, \\ \tilde{\mathcal{C}} &= C_1 V - C_2 (A_3 M^{-1} A_2)^{-1} A_3 M^{-1} (A_1 V), \\ \tilde{\mathcal{D}} &= D - C_2 (A_3 M^{-1} A_2)^{-1} A_3 M^{-1} B_1. \end{aligned} \quad (22)$$

Here, the projection matrices  $V$  and  $W$  are composed of suitable sparsity-preserving matrix-vector formulation. The ROM corresponding to the reduced-order matrices defined in (22) can be written as follows:

$$\begin{aligned} \tilde{\mathcal{E}} \dot{x}(t) &= \tilde{\mathcal{A}} x(t) + \tilde{\mathcal{B}} u(t), \\ y(t) &= \tilde{\mathcal{C}} x(t) + \tilde{\mathcal{D}} u(t). \end{aligned} \quad (23)$$

### 3. Two-Sided Iterative Algorithm for Index-2 Descriptor Systems

This section includes the main tasks of this work. We derive an improved version of the two-sided iterative algorithm (TSIA) for index-2 descriptor systems to stabilize the incompressible Navier–Stokes flow.

*3.1. Formulation of the Generalized Sparse-Dense Sylvester Equation.* Initially, we assume a makeshift ROM with the desired dimension in the form (23) employing any classical iterative method accomplishing a few iterations. However, due to the use of a minimum number of iterations, the attained ROM cannot efficiently approximate the original system. So, the quality of the ROM needs to be improved by further techniques such that it satisfies the Wilson conditions for  $\mathcal{H}_2$  optimality [42, 47].

Now, we are to construct two generalized sparse-dense Sylvester equations. To do this, we need to compute the following matrices:

$$\begin{aligned} B_n &= \begin{bmatrix} M & A_2 \\ A_3 & 0 \end{bmatrix}^{-1} \begin{bmatrix} B_1 \\ B_2 \end{bmatrix}, \\ C_n &= \begin{bmatrix} M^T & A_3^T \\ A_2^T & 0 \end{bmatrix}^{-1} \begin{bmatrix} C_1^T \\ C_2^T \end{bmatrix}. \end{aligned} \quad (24)$$

Assuming  $P_n = MB_n\tilde{\mathcal{B}}^T$  and  $Q_n = -MC_n\tilde{\mathcal{E}}$ , the required sparse-dense Sylvester equations can be formed as follows:

$$\begin{aligned} \mathcal{A}X\tilde{\mathcal{E}} + \mathcal{E}X\tilde{\mathcal{A}} + P_n &= 0, \\ \mathcal{A}Y\tilde{\mathcal{E}} + \mathcal{E}Y\tilde{\mathcal{A}} + Q_n &= 0. \end{aligned} \quad (25)$$

**3.2. Solving the Generalized Sparse-Dense Sylvester Equation.** Sylvester equations formed in formula (25) can be solved by the techniques given in Section 3.2 of reference [48]. Since the simulations of the Sylvester equations in formula (25) are analogous, we will derive the method for computing  $X$  only. To generate the Krylov subspace QZ-decomposition of  $\tilde{\mathcal{E}}$  and  $\tilde{\mathcal{A}}$  is to be computed, such that  $\tilde{\mathcal{E}} = QSZ^T$  and  $\tilde{\mathcal{A}} = QTZ^T$ , respectively. Here,  $S$  and  $T$  are the upper triangular matrices. As the techniques provided in reference [48] of the dense form, we have to rewrite the basis vector in the sparse form as follows:

$$\begin{bmatrix} S_{jj}A_1 + T_{jj}M^T & S_{jj}A_2 \\ S_{jj}A_3 & 0 \end{bmatrix} \tilde{X}_j = -\tilde{P}_n^{(j)}, \quad (26)$$

and the successive columns for the solution matrix  $X$  can be generated as follows:

$$\tilde{P}_n^{(j)} = -\tilde{P}_n^{(j)} - \sum_{i=1}^{j-1} F_{ij}\tilde{X}_i, \quad (27)$$

where  $\tilde{P}_n^{(j)} = P_n^{(j)}Z$  and  $F_{ij} = \begin{bmatrix} S_{ij}A_1 + T_{ij}M^T & S_{ij}A_2 \\ S_{ij}A_3 & 0 \end{bmatrix}$ . The updated sparse form of the desired techniques are provided in Algorithm 5.

**3.3. Two-Sided Iterative Algorithm to Estimate the Optimal Feedback Matrix.** At first, an iterative method with minimum iterations needs to be utilized to find an initial makeshift ROM with the desired dimension. With the required matrix-vector algebraic operations, the Sylvester equations defined in formula (25) need to be solved for  $X$  and  $Y$ , respectively. Then, the approximated projector matrices  $\tilde{V}$  and  $\tilde{W}$  can be computed by the QR-decomposition of the matrices  $X$  and  $Y$ , respectively. Those crude projector matrices need to be refined as  $V = \tilde{V}$  and  $W = \tilde{W}(\tilde{V}^T M^T \tilde{W})^{-1}$ , respectively. Implementing  $V$  and  $W$  the ROM (23) can be acquired with the reduced-order matrices defined in formula (22); hence, the reduced-order Riccati equation can be formed as follows:

$$\tilde{\mathcal{A}}^T \tilde{X} \tilde{\mathcal{E}} + \tilde{\mathcal{E}}^T \tilde{X} \tilde{\mathcal{A}} - \tilde{\mathcal{E}}^T \tilde{X} \tilde{\mathcal{B}} \tilde{\mathcal{B}}^T \tilde{X} \tilde{\mathcal{E}} + \tilde{\mathcal{E}}^T \tilde{\mathcal{E}} = 0, \quad (28)$$

which can be solved for  $\tilde{X}$  by MATLAB *care* command, and then, the reduced-order feedback matrix can be estimated as  $\tilde{K} = \tilde{\mathcal{B}}^T \tilde{X} \tilde{\mathcal{E}}$ . Finally, the optimal feedback matrix for system (1) can be approximated as follows:

$$K^o = \left( \tilde{\mathcal{B}}^T \tilde{X} \tilde{\mathcal{E}} \right) V^T \tilde{\mathcal{E}} = \tilde{K} V^T M. \quad (29)$$

The whole process is summed up in Algorithm 6.

**3.4. Stabilization of the Index-2 Descriptor System.** Plugging the optimal feedback matrix  $K^o$ , the unstable incompressible Navier–Stokes flow given by (1) can be optimally stabilized as follows:

$$\begin{aligned} M\dot{v}(t) &= (A_1 - B_1 K^o)v(t) + A_2 p(t) + B_1 u(t), \\ 0 &= A_3 v(t) + B_2 u(t), \\ y(t) &= C_1 v(t) + C_2 p(t) + Du(t). \end{aligned} \quad (30)$$

**3.5.  $\mathcal{H}_2$  Norm of the Error System.** Let us consider  $G(s)$  and  $\tilde{G}(s)$  are the transfer functions of the converted generalized system (15) and (23), respectively. Then, the associated error system can be formulated as follows:

$$G_{err} = G(s) - \tilde{G}(s) = \mathcal{E}_{err} (s\mathcal{E}_{err} - \mathcal{A}_{err})^{-1} \mathcal{B}_{err}, \quad (31)$$

where we have taken the reduced-order matrices of formula (22) into account and the system matrices are formed as follows:

$$\begin{aligned} \mathcal{E}_{err} &= \begin{bmatrix} \mathcal{E} & 0 \\ 0 & \tilde{\mathcal{E}} \end{bmatrix}, \quad \mathcal{A}_{err} = \begin{bmatrix} \mathcal{A} & 0 \\ 0 & \tilde{\mathcal{A}} \end{bmatrix}, \\ \mathcal{B}_{err} &= \begin{bmatrix} \mathcal{B} \\ \tilde{\mathcal{B}} \end{bmatrix}, \quad \text{and } \mathcal{C}_{err} = \begin{bmatrix} \mathcal{C} & -\tilde{\mathcal{C}} \end{bmatrix}. \end{aligned} \quad (32)$$

Authors in reference [49] derived the way of estimating  $\mathcal{H}_2$  norm of the error system (31) as follows:

$$\|G_{err}\|_{\mathcal{H}_2} = \sqrt{\|G(s)\|_{\mathcal{H}_2}^2 + \|\tilde{G}(s)\|_{\mathcal{H}_2}^2 + 2\text{trace}(\mathcal{B}^T \mathcal{Q}_s \tilde{\mathcal{B}})}. \quad (33)$$

Here,  $\mathcal{H}_2$  norm of the full model is defined as  $\|G(s)\|_{\mathcal{H}_2}$  and needs to be evaluated for once, which is inconvenient for the conventional simulation solvers. Assuming  $Z_q$  is the low-rank Gramian factor of the Gramian  $\mathcal{Q}$  that needs to be determined. In reference [50], a practically feasible technique is derived to overcome this situation. Then,  $\|G(s)\|_{\mathcal{H}_2}$  can be written as follows:

$$\|G(s)\|_{\mathcal{H}_2} = \sqrt{\text{trace}\left((B_1^T Z_q)(B_1^T Z_q)^T + (B_2^T Z_q)(B_2^T Z_q)^T\right)}. \quad (34)$$

Again,  $\|\tilde{G}(s)\|_{\mathcal{H}_2}$  is the  $\mathcal{H}_2$  norm of the ROM that can be evaluated by the Gramian  $\tilde{\mathcal{Q}}$  of the low-rank Lyapunov equation

$$\tilde{\mathcal{A}}^T \tilde{\mathcal{Q}} \tilde{\mathcal{E}} + \tilde{\mathcal{E}}^T \tilde{\mathcal{Q}} \tilde{\mathcal{A}} + \tilde{\mathcal{E}}^T \tilde{\mathcal{E}} = 0, \quad (35)$$

Input:  $M, A_1, A_2, A_3, B_1, B_2, \tilde{\mathcal{E}}, \tilde{\mathcal{A}}, \tilde{\mathcal{B}}, j_{\max}$  (number of iterations).  
Output: approximate solution  $X$  of the Sylvester (25).  
(1) Compute the QZ-decomposition  $\tilde{\mathcal{E}} = QSZ^T$  and  $\tilde{\mathcal{A}} = QTZ^T$ .  
(2) Construct  $B_n$  according to (24) and compute  $P_n = MB_n\tilde{\mathcal{B}}^T$ .  
(3) Compute  $\tilde{P}_n = P_nZ$ .  
(4) while  $j \leq j_{\max}$  do  
(5) Compute  $\tilde{P}_n^{(j)}$  by formula (27).  
(6) Solve the linear system (26) for  $\tilde{X}_j$ .  
(7) end while  
(8) Compute  $X = \tilde{X}Q^T$ .

ALGORITHM 5: Solution of generalized sparse-dense Sylvester equation.

Input:  $M, A_1, A_2, A_3, B_1, B_2, C_1, C_2, \tilde{\mathcal{E}}, \tilde{\mathcal{A}}, \tilde{\mathcal{B}}, \tilde{\mathcal{C}}$   
Output:  $\tilde{\mathcal{E}}, \tilde{\mathcal{A}}, \tilde{\mathcal{B}}, \tilde{\mathcal{C}}$  satisfying the Wilson conditions.  
(1) Construct the Sylvester equations defined in (25) and solve for  $X$  and  $Y$ , respectively.  
(2) Compute the QR decomposition  $X = \tilde{V}\beta_v$  and  $Y = \tilde{W}\beta_w$ .  
(3) Compute  $V = \tilde{V}$  and  $W = \tilde{W}(\tilde{V}^T M^T \tilde{W})^{-1}$ .  
(4) Construct the Wilson conditions satisfying reduced-order matrices defined in (22).  
(5) Form the reduced-order Riccati (28) and solve for  $\tilde{X}$ .  
(6) Approximate the optimal feedback matrix from (29).

ALGORITHM 6: TSIA for the optimal feedback matrix of index-2 descriptor systems.

due to the involvement of the reduced-order matrices, the Lyapunov (35) is solvable by the MATLAB library command *lyap*.

Finally,  $\text{trace}(\mathcal{B}^T \mathcal{Q}_s \tilde{\mathcal{B}})$  can be computed by the Gramian  $\mathcal{Q}_s$  of the sparse-dense Sylvester equation

$$\mathcal{A}^T \mathcal{Q}_s \tilde{\mathcal{E}} + \tilde{\mathcal{E}}^T \mathcal{Q}_s \tilde{\mathcal{A}} + \tilde{\mathcal{E}}^T \tilde{\mathcal{C}} = 0, \quad (36)$$

that can be conveniently solved by reforming the techniques provided in Algorithm 5.

## 4. Numerical Results

In this section, the justification of the adaptability and efficiency of the proposed techniques will be discussed. Computations are performed through MATLAB simulations to observe the betterment of the proposed techniques in comparison to the present methods. The investigation involves both the graphical and tabular approaches. Computation time and accuracy of the approximation, and robustness of the stabilization of the transient behaviors will be the prime concern of this discussion. We have implemented the proposed techniques to the real-world Navier–Stokes models of unstable type.

All the results have been achieved using MATLAB 8.5.0 (R2015a) on a Windows machine having Intel-Xeon Silver 4114 CPU 2.20 GHz clock speed, 2 cores each, and 64 GB of total RAM.

**4.1. Model Description.** In this work, we have considered some unstable Navier–Stokes models with the Reynolds number  $Re = 300, 400, 500$ , respectively. The dimension of the models varies from 1 to 5. Each of the models is non-symmetric having 2 inputs with 7 outputs. For the target models, in the conventional first-order index-2 descriptor

system the submatrices  $B_2$  and  $C_2$  both are the sparse zero matrices. The full specifications of the target models are given in Table 1.

**4.2. Approximation of the Full Models with the Reduced-Order Models.** The accuracy of the approximation of the full models with the ROMs will be validated here. We will verify the level of approximation graphically and then evaluate the  $\mathcal{H}_2$ -norm of the error systems for the objective models.

**4.3. Comparison of the Transfer Functions.** A graphical comparison between the full models and ROMs will be depicted. Since the Navier–Stokes models of various dimensions have the same system structure and transitional properties in the graphical analysis, we will only show the properties of the 3-dimensional model with  $Re = 500$ .

In Figure 1, the subfigure Figure 1(a) shows the comparison of the transfer function (sigma plot) of the full model and corresponding ROM, whereas subfigures Figures 1(b) and 1(c) evince the absolute and relative errors, respectively, of this reduced-order approximation. From the abovementioned figures, it can be evident that by the proposed techniques the objective full models can be properly approximated by the ROMs with a reasonable level of accuracy.

**4.4.  $\mathcal{H}_2$  Norm of the Error System for the ROMs.** Here,  $\mathcal{H}_2$  norm of the error system for the ROMs of the target models will be provided.

TABLE 1: Structure of the target Navier–Stokes models.

Dimension	Reynolds number (Re)	States	Algebraic variables	Input	Output
1	300	3142	453		
	400				
	500				
2	300	8568	1123		
	400				
	500				
3	300	19770	2615	2	7
	400				
	500				
4	300	44744	5783		
	400				
	500				
5	300	98054	12566		
	400				
	500				

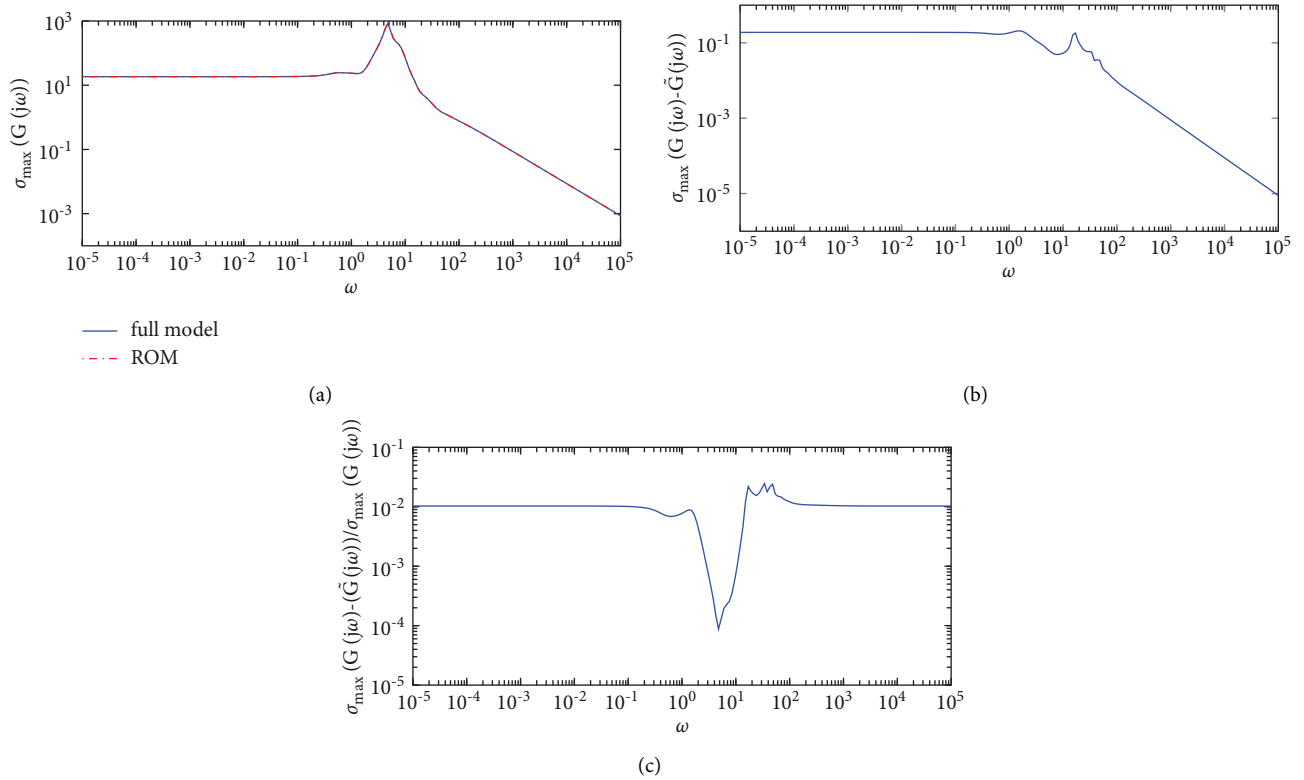


FIGURE 1: Comparison of full model and ROM of 3-dimensional model for Re = 500. (a) Sigma plot. (b) Absolute error. (c) Relative error.

Table 2 conveys the desired  $\mathcal{H}_2$  error norm of the ROMs. From the measured  $\mathcal{H}_2$  error norm of the ROMs, it is evident that the level of the approximation process is suitably robust and confirms the compatible scale of the accuracy.

**4.5. Graphical Validation of Stabilization of the Unstable Systems.** In this section, the stabilization of the unstable Navier–Stokes models will be graphically illustrated. For the

compactness of this article, we will only demonstrate the stabilization of the transient behaviors of the 3-dimensional models.

**4.6. Stabilization of the Eigenvalues.** The subfigures of Figure 2 exhibit the eigenvalues of the original (unstable) 3-dimensional systems with Reynolds number Re = 300, 400, 500, respectively. In contrast, the subfigures of

TABLE 2:  $\mathcal{H}_2$  error norm of the ROMs of the target models.

Reynolds Number	Dimension	$\mathcal{H}_2$ error norm
300	1	$2.11 \times 10^{-03}$
	2	$7.52 \times 10^{-04}$
	3	$7.90 \times 10^{-04}$
	4	$8.12 \times 10^{-04}$
	5	$8.49 \times 10^{-04}$
400	1	$1.55 \times 10^{-02}$
	2	$3.25 \times 10^{-03}$
	3	$3.57 \times 10^{-03}$
	4	$3.95 \times 10^{-03}$
	5	$4.15 \times 10^{-03}$
500	1	$2.62 \times 10^{-01}$
	2	$1.22 \times 10^{-02}$
	3	$1.74 \times 10^{-02}$
	4	$1.88 \times 10^{-02}$
	5	$9.46 \times 10^{-03}$

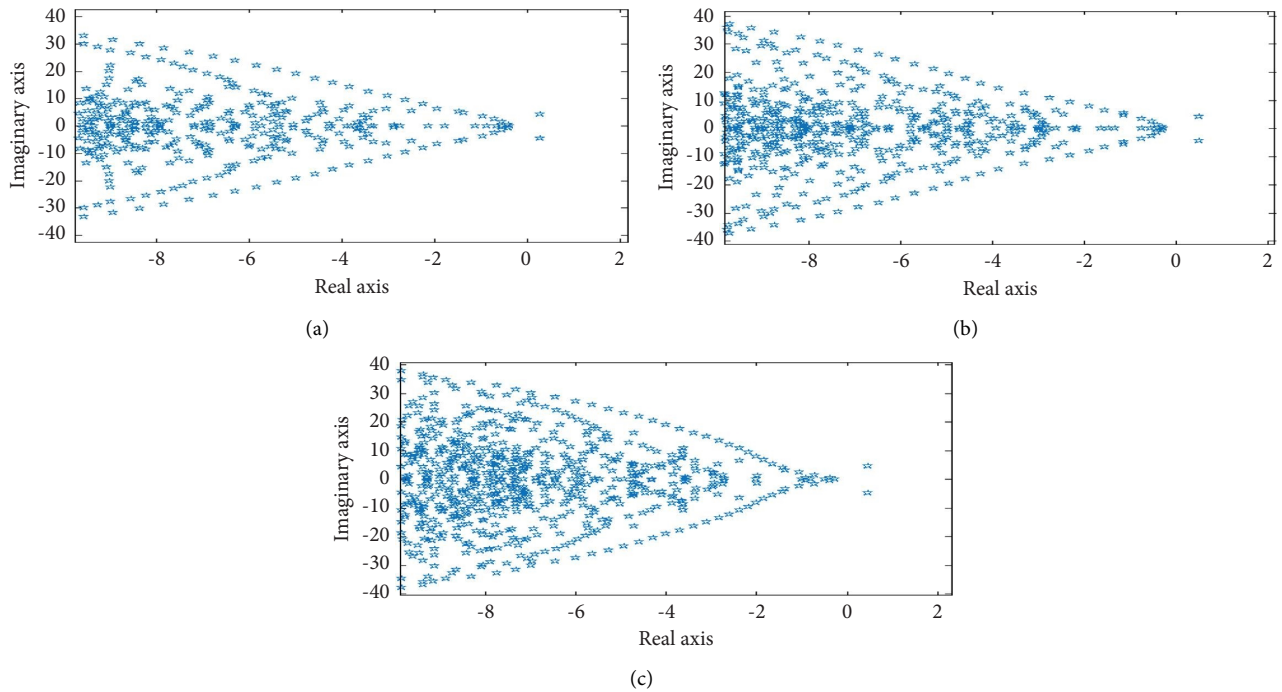


FIGURE 2: Unstable eigenvalues of 3-dimensional models. (a) Reynolds number 300. (b) Reynolds number 400. (c) Reynolds number 500.

Figure 3 exhibit the stabilized eigenvalues of that of the systems. From those figures, it can be concluded that the eigenvalues of the desired models are properly stabilized.

4.7. *Stabilization of the Step Responses.* The subfigure of Figures 4 and 5 display the step-responses of the 1st-input/1st-output and 2nd-input/7th-output relations, respectively, of the abovementioned original (unstable) systems. On the contrary, the subfigures of Figures 6 and 7 display the stabilized step responses of the 1st-input/1st-output and 2nd-input/7th-output relations, respectively, of that the systems. The scenario of the step-response stabilization duly confirms the efficiency of the proposed techniques.

4.8. *Comparison of the TSIA with IRKA.* In this section, we are going to compare the proposed algorithm with the IRKA approach for reduced-order modelling. Initially, we aimed to compare with the RKSM approach as well. However, due to the nonsymmetric structure of the Navier–Stokes models, the RKSM approach is applicable for here. Since the stabilization of the eigenvalues and step-responses by the TSIA and IRKA via the reduced-order modeling is very identical, we have ignored their graphical comparisons and chosen the tabular comparisons. In this comparative analysis, we will investigate both of the computation time and the  $\mathcal{H}_2$  error norm of the ROMs of selected 3-dimensional models. Table 3 reveals the required information on computation time and  $\mathcal{H}_2$  error norm.

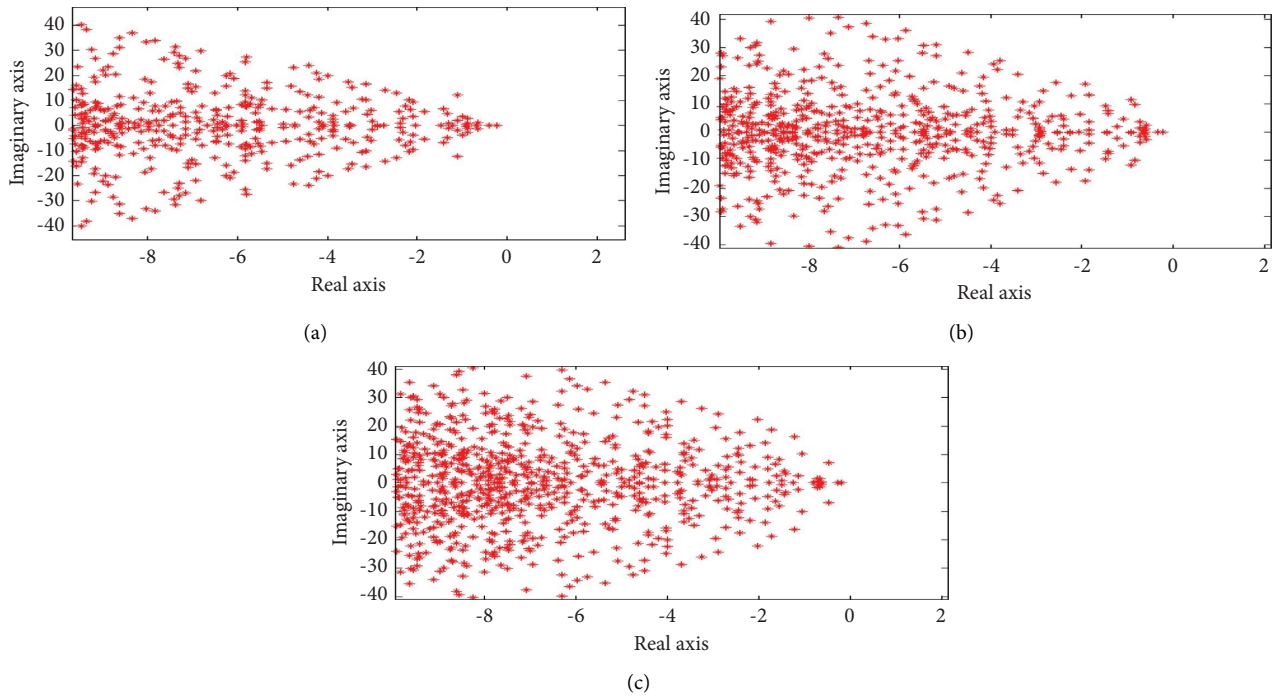


FIGURE 3: Stabilized eigenvalues of 3-dimensional models. (a) Reynolds number 300. (b) Reynolds number 400. (c) Reynolds number 500.

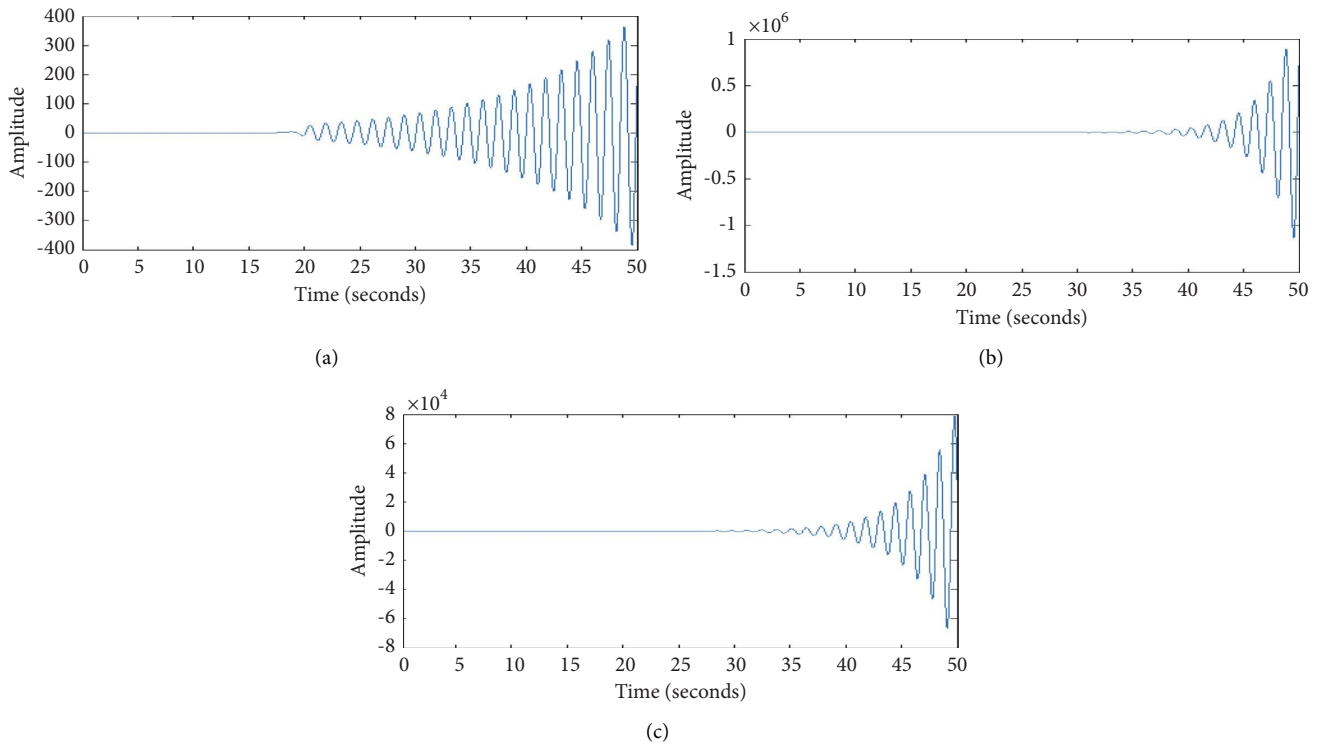


FIGURE 4: Unstable step response for 1st input/1st output of 3-dimensional models. (a) Reynolds number 300. (b) Reynolds number 400. (c) Reynolds number 500.

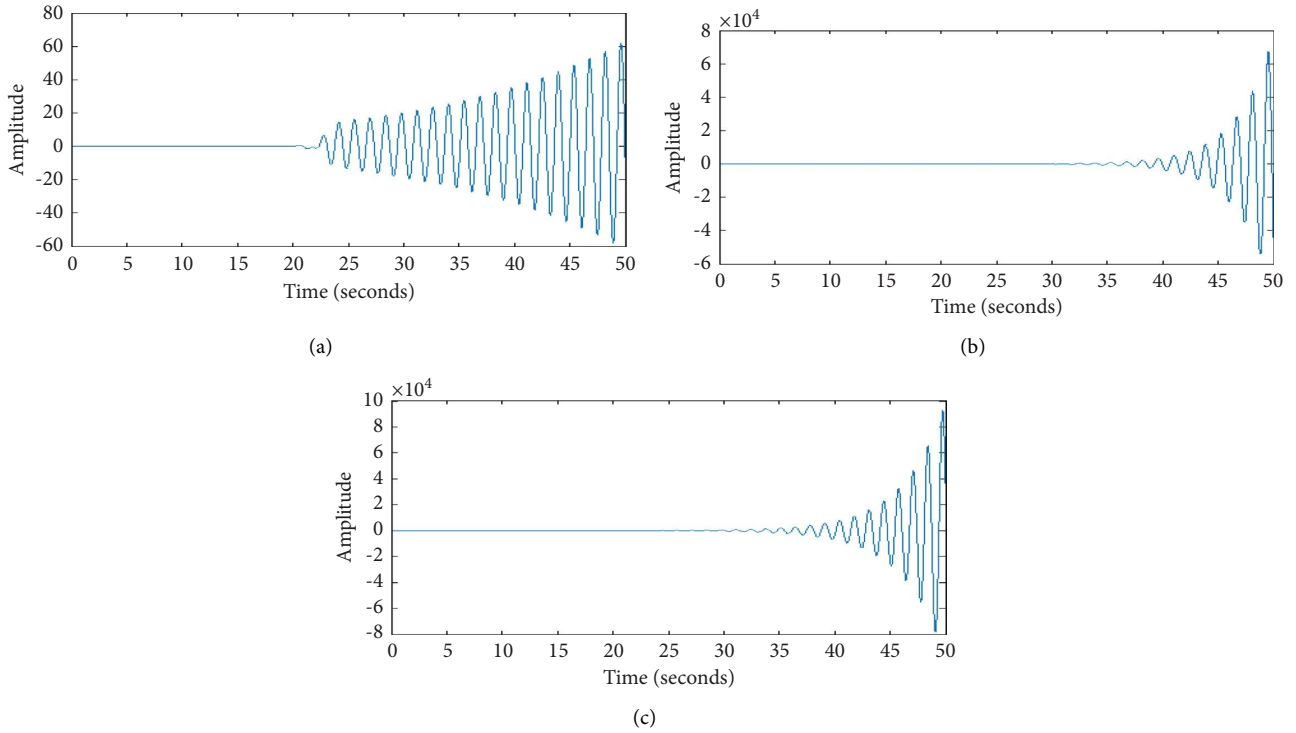


FIGURE 5: Unstable step response for 2nd input/7th output of 3-dimensional models. (a) Reynolds number 300. (b) Reynolds number 400. (c) Reynolds number 500.

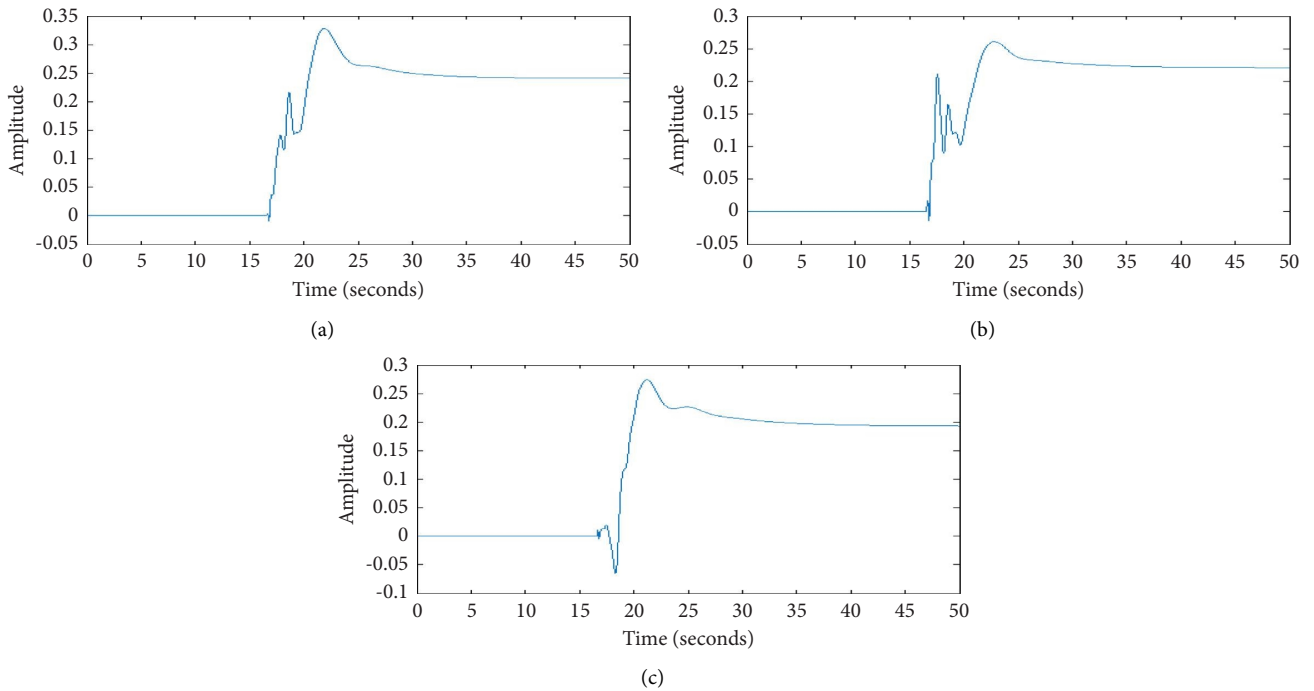


FIGURE 6: Stabilized step response for 1st input/1st output of 3-dimensional models. (a) Reynolds number 300. (b) Reynolds number 400. (c) Reynolds number 500.

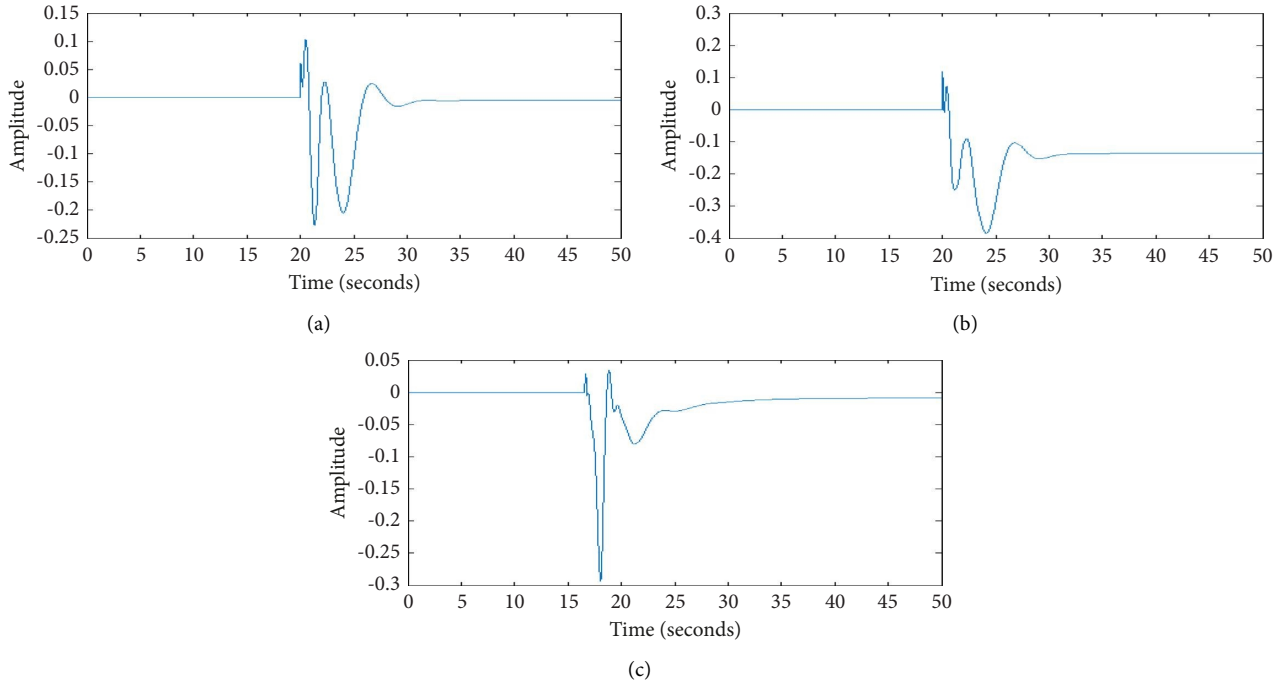


FIGURE 7: Stabilized step response for 2nd input/7th output of 3-dimensional models. (a) Reynolds number 300. (b) Reynolds number 400. (c) Reynolds number 500.

TABLE 3: Comparison of computation time and  $\mathcal{H}_2$  error norm of the ROMs of 3-dimensional models archived by TSIA and IRKA.

Reynolds Number	Time		$\mathcal{H}_2$ error norm	
	TSIA	IRKA	TSIA	IRKA
300	$6.81 \times 10^3$	$9.83 \times 10^3$	$7.90 \times 10^{-04}$	$9.97 \times 10^{-04}$
400	$6.86 \times 10^3$	$9.65 \times 10^3$	$3.57 \times 10^{-03}$	$6.30 \times 10^{-03}$
500	$6.94 \times 10^3$	$9.68 \times 10^3$	$1.74 \times 10^{-02}$	$5.13 \times 10^{-02}$

From Table 3, it is apparent that in the case of computation time, the TSIA algorithm requires about two-thirds of that of IRKA. Also, a comparison of  $\mathcal{H}_2$  error norm of the ROMs manifests the betterment of TSIA over IRKA.

## 5. Conclusions

We have introduced a two-sided projection-based sparsity-preserving reduced-order modeling approach for the stabilization of nonsymmetric index-2 descriptor systems explored from unstable Navier–Stokes models. The Wilson conditions satisfying Reduced-order models are derived by the two-sided projection techniques implementing the sparse-dense Sylvester equations. To solve the desired Sylvester equations, sparsity-preserving Krylov subspaces are structured via the system of linear equations with a compact form of matrix-vector operations. From the numerical analyses, it is ascertained that the proposed techniques can be proficiently applied for the stabilization of the target models through reduced-order modeling. We have efficiently approximated the full models by the corresponding ROMs with minimized  $\mathcal{H}_2$  error norm and stabilized the eigenvalues and step-responses properly. A comparison of reduced-order modelling by TSIA and IRKA is performed. From the comparative discussion, it is

manifested that the techniques involved in TSIA outplayed that of the IRKA in both the saving computation time and  $\mathcal{H}_2$  error norm. Also, we intended to include RKSM in the comparative analysis but found that RKSM is not applicable to the target models due to the nonsymmetric structure. Thus, the bottom line of the article is that the proposed techniques can be utilized to stabilize the unstable Navier–Stokes models with better accuracy and less computing time.

## Data Availability

The computational data of the Navier–Stokes models are available at <https://github.com/uddinmonir/systemDATA/find/main>.

## Conflicts of Interest

The authors declare that they have no conflicts of interest.

## Acknowledgments

This research work was funded by an NSU-CTRG research grant under project no.: CTRG-19/SEPS/05.

## References

- [1] S. Ravindran, “Stabilization of Navier-Stokes equations by boundary feedback,” *International Journal of Numerical Analysis and Modeling*, vol. 4, no. 3-4, pp. 608–624, 2007.
- [2] E. Bänsch, P. Benner, J. Saak, and H. K. Weichelt, “Riccati-based boundary feedback stabilization of incompressible Navier–Stokes flows,” *SIAM Journal on Scientific Computing*, vol. 37, no. 2, pp. 832–858, 2015.

- [3] R. Altmann and J. Heiland, "Continuous, Semi-discrete, and Fully Discretised Navier-Stokes Equations," *Applications of Differential-Algebraic Equations: Examples and Benchmarks*, p. 277, 2018.
- [4] E. Bänsch, P. Benner, J. Saak, and H. K. Weichelt, "Optimal control-based feedback stabilization of multi-field flow problems," *Trends in PDE Constrained Optimization*, pp. 173–188, Springer, New York, NY, USA, 2014.
- [5] J. T. Borggaard and S. Gugercin, "Model reduction for DAEs with an application to flow control," *Active Flow and Combustion Control*, vol. 127, p. 381, 2014.
- [6] V. Mehrmann and T. Stykel, *Balanced Truncation Model Reduction for Large-Scale Systems in Descriptor Form*, Springer, New York, NY, USA, 2005.
- [7] F. Gargano, M. Sammartino, V. Sciacca, and K. W. Cassel, "Analysis of complex singularities in high-Reynolds-number Navier–Stokes solutions," *Journal of Fluid Mechanics*, vol. 747, pp. 381–421, 2014.
- [8] M. Uddin, J. Saak, and P. Benner, "Balancing based model reduction for structured index-2 unstable descriptor systems with application to flow control," *Numerical Algebra, Control and Optimization*, vol. 6, no. 1, pp. 1–20, 2016.
- [9] J. P. Raymond, "Local boundary feedback stabilization of the Navier-Stokes equations," *Control Systems: Theory, Numerics and Applications*, vol. 30, 2005.
- [10] P. Benner, Z. Bujanović, P. Kürschner, and J. Saak, "A numerical comparison of different solvers for large-scale, continuous-time algebraic Riccati equations and LQR problems," *SIAM Journal on Scientific Computing*, vol. 42, no. 2, pp. 957–996, 2020.
- [11] A. C. Antoulas, "An overview of approximation methods for large-scale dynamical systems," *Annual Reviews in Control*, vol. 29, no. 2, pp. 181–190, 2005.
- [12] P. Benner and T. Stykel, "Model order reduction for differential-algebraic equations: a survey," *Surveys in Differential-Algebraic Equations IV*, p. 107, Springer, New York, NY, USA, 2017.
- [13] P. Benner, M. Heinkenschloss, J. Saak, and H. K. Weichelt, "Efficient solution of large-scale algebraic Riccati equations associated with index-2 DAEs via the inexact low-rank Newton-ADI method," *Applied Numerical Mathematics*, vol. 152, pp. 338–354, 2020.
- [14] G. M. Flagg, C. A. Beattie, and S. Gugercin, "Convergence of the iterative rational Krylov algorithm," *Systems & Control Letters*, vol. 61, no. 6, pp. 688–691, 2012.
- [15] P. Benner, P. Kürschner, and J. Saak, "An improved numerical method for balanced truncation for symmetric second-order systems," *Mathematical and Computer Modelling of Dynamical Systems*, vol. 19, no. 6, pp. 593–615, 2013.
- [16] P. Benner, S. Gugercin, and K. Willcox, "A survey of projection-based model reduction methods for parametric dynamical systems," *SIAM Review*, vol. 57, no. 4, pp. 483–531, 2015.
- [17] M. Sahadet Hossain and M. Monir Uddin, "Reduce order modelling of power system models using interpolatory projections technique," *International Journal of Modeling and Optimization*, vol. 5, no. 3, pp. 228–233, 2015.
- [18] K. Sinani, *Iterative Rational Krylov Algorithm for Unstable Dynamical Systems and Generalized Coprime Factorizations*, Ph.D. dissertation, Virginia Tech, Virginia, VA, USA, 2016.
- [19] P. Benner, J. Saak, and M. M. Uddin, "Reduced-order modeling of index-1 vibrational systems using interpolatory projections," in *Proceedings of the 2016 19th International Conference on Computer and Information Technology (ICCIT)*, pp. 134–138, IEEE, Dhaka, Bangladesh, December 2016.
- [20] M. Uddin, M. M. Uddin, M. H. Khan, and M. M. Rahman, "Interpolatory projection technique for Riccati-based feedback stabilization of index-1 descriptor systems," in *IOP Conference Series: Materials Science and Engineering* vol. 1070, no. 1, p. 012, IOP Publishing, 2021.
- [21] M. M. Rahman, M. M. Uddin, L. S. Andallah, and M. Uddin, "Tangential interpolatory projections for a class of second-order index-1 descriptor systems and application to mechatronics," *Production Engineering*, vol. 15, no. 1, pp. 9–19, 2021.
- [22] V. Druskin and V. Simoncini, "Adaptive rational krylov subspaces for large-scale dynamical systems," *Systems & Control Letters*, vol. 60, no. 8, pp. 546–560, 2011.
- [23] T. Stykel and V. Simoncini, "Krylov subspace methods for projected Lyapunov equations," *Applied Numerical Mathematics*, vol. 62, no. 1, pp. 35–50, 2012.
- [24] Y. Lin and V. Simoncini, "A new subspace iteration method for the algebraic Riccati equation," *Numerical Linear Algebra with Applications*, vol. 22, no. 1, pp. 26–47, 2015.
- [25] M. Uddin, M. M. Uddin, and M. A. Hakim Khan, "Computationally efficient optimal control for unstable power system models," *Mathematical Problems in Engineering*, vol. 2021, Article ID 8071869, 17 pages, 2021.
- [26] H. Mena and J. Saak, "On the parameter selection problem in the Newton-ADI iteration for large-scale Riccati equations," *Electronic Transactions on Numerical Analysis*, vol. 29, pp. 136–149, 2008.
- [27] F. Feitzinger, T. Hylla, and E. W. Sachs, "Inexact Kleinman-Newton method for Riccati equations," *SIAM Journal on Matrix Analysis and Applications*, vol. 31, no. 2, pp. 272–288, 2009.
- [28] P. Benner and T. Stykel, "Numerical solution of projected algebraic Riccati equations," *SIAM Journal on Numerical Analysis*, vol. 52, no. 2, pp. 581–600, 2014.
- [29] D. Palitta, "The Projected newton-kleinman Method for the Algebraic Riccati Equation," 2019, <https://arxiv.org/abs/1901.10199>.
- [30] E. Bänsch and P. Benner, "Stabilization of incompressible flow problems by Riccati-based feedback," *constrained optimization and optimal control for partial differential equations*, vol. 160, pp. 5–20, 2012.
- [31] J. Cullum and T. Zhang, "Two-sided Arnoldi and nonsymmetric Lanczos algorithms," *SIAM Journal on Matrix Analysis and Applications*, vol. 24, no. 2, pp. 303–319, 2002.
- [32] P. Benner and T. Breiten, "Two-sided projection methods for nonlinear model order reduction," *SIAM Journal on Scientific Computing*, vol. 37, no. 2, pp. 239–260, 2015.
- [33] I. V. Gosea and A. C. Antoulas, "A two-sided iterative framework for model reduction of linear systems with quadratic output," in *Proceedings of the 2019 IEEE 58th Conference on Decision and Control (CDC)*, pp. 7812–7817, Nice, France, December 2019.
- [34] J. Yuan, R. J. B. De Sampato, and D. J. Evans, "Applications of QZ decomposition," *International Journal of Computer Mathematics*, vol. 60, no. 1-2, pp. 105–114, 1996.
- [35] T. Hylla, *Extension of Inexact Kleinman-Newton Methods to a General Monotonicity Preserving Convergence Theory*, Ph.D. Thesis, Universität Trier, Trier, Germany, 2011.
- [36] J. R. Li, *Model Reduction of Large Linear Systems via Low Rank System Gramians*, Ph.D. dissertation, Massachusetts Institute of Technology, Massachusetts, MA, USA, 2000.
- [37] P. Benner, P. Kürschner, and J. Saak, "Efficient handling of complex shift parameters in the low-rank Cholesky factor

- ADI method,” *Numerical Algorithms*, vol. 62, no. 2, pp. 225–251, 2013.
- [38] M. M. Uddin, *Computational Methods for Approximation of Large-Scale Dynamical Systems*, Chapman and Hall/CRC, Boca Raton, Florida, 2019.
- [39] V. Simoncini, D. B. Szyld, and M. Monsalve, “On two numerical methods for the solution of large-scale algebraic Riccati equations,” *IMA Journal of Numerical Analysis*, vol. 34, no. 3, pp. 904–920, 2013.
- [40] V. Simoncini, “Analysis of the rational Krylov subspace projection method for large-scale algebraic Riccati equations,” *SIAM Journal on Matrix Analysis and Applications*, vol. 37, no. 4, pp. 1655–1674, 2016.
- [41] M. Uddin, “Numerical Study on Continuous-Time Algebraic Riccati Equations Arising from Large-Scale Sparse Descriptor Systems,” Master’s Thesis, Bangladesh University of Engineering and Technology, Bangladesh, India, 2020.
- [42] S. Gugercin, A. C. Antoulas, and C. Beattie, “ $\mathcal{H}_2$  model reduction for large-scale linear dynamical systems,” *SIAM Journal on Matrix Analysis and Applications*, vol. 30, no. 2, pp. 609–638, 2008.
- [43] A. C. Antoulas, C. A. Beattie, and S. Gugercin, *Interpolatory Model Reduction of Large-Scale Dynamical Systems*, Springer, New York, NY, USA, 2010.
- [44] M. Heinkenschloss, D. C. Sorensen, and K. Sun, “Balanced truncation model reduction for a class of descriptor systems with application to the Oseen equations,” *SIAM Journal on Scientific Computing*, vol. 30, no. 2, pp. 1038–1063, 2008.
- [45] S. Gugercin, T. Stykel, and S. Wyatt, “Model reduction of descriptor systems by interpolatory projection methods,” *SIAM Journal on Scientific Computing*, vol. 35, no. 5, pp. 1010–1033, 2013.
- [46] S. Wyatt, *Issues in Interpolatory Model Reduction: Inexact Solves, Second-Order Systems and DAEs*, Ph.D. dissertation, Virginia Tech, Virginia, VA, USA, 2012.
- [47] K.-L. Xu and Y.-L. Jiang, “Reduced optimal models via cross Gramian for continuous linear time-invariant systems,” *IET Circuits, Devices and Systems*, vol. 12, no. 1, pp. 25–32, 2018.
- [48] P. Benner, M. Köhler, and J. Saak, “Sparse-dense Sylvester Equations in  $\mathcal{H}_2$ -Model Order Reduction,” 2011, <https://arxiv.org/pdf/2108.03312.pdf>.
- [49] M. M. Rahman, M. M. Uddin, L. S. Andallah, and M. Uddin, “Interpolatory projection techniques for  $\mathcal{H}_2$  optimal structure-preserving model order reduction of second-order systems,” *Advances in Science, Technology and Engineering Systems Journal*, vol. 5, no. 4, pp. 715–723, 2020.
- [50] M. Uddin, M. M. Uddin, M. A. H. Khan, and M. T. Hossain, “SVD-Krylov based sparsity-preserving techniques for Riccati-based feedback stabilization of unstable power system models,” *Journal of Engineering Advancements*, vol. 2, no. 3, pp. 125–131, 2021.